

Resonant magnetoexcitons and the Fermi-edge singularity in a magnetic field

Pawel Hawrylak

Institute for Microstructural Sciences, National Research Council of Canada, Ottawa, Canada, K1A 0R6

(Received 4 February 1991)

The effect of the magnetic field B on the Fermi-edge singularity in optical properties of asymmetric quantum wells is investigated using a two-subband Mahan–Nozières–De Dominicis Hamiltonian. The emission spectrum for carriers in the lowest subband is strongly enhanced by excitonic transitions involving higher subbands. The modulation of the emission spectrum is almost periodic in $1/B$.

The problem of optical transitions in the presence of an electron gas has been extensively studied.¹ Recent interest concentrated on artificially structured semiconductor microstructures with a tunable electron density: gated heterojunctions,² modulation-doped quantum wells,^{3–6} and double-barrier resonant-tunneling structures.⁷ The enhancement of the emission spectrum in the vicinity of the Fermi level [Fermi-edge singularity (FES)] has been observed by Skolnick *et al.*³ It was argued that the localization of holes allowed the observation of FES. For extended hole states the FES is expected to be reduced in the emission spectrum.⁸ Recent experiments by Chen *et al.*⁹ on asymmetric quantum wells enhance the FES by coupling it with excitons associated with higher subbands. The large enhancement of the emission spectrum in the vicinity of the Fermi level has been shown experimentally and calculated theoretically.¹⁰ The application of the magnetic field led to dramatic changes in the emission spectrum⁹ in the energy range corresponding to the overlap of the magnetoexciton associated with the second subband and the Fermi level in the first subband.

We present here a calculation of the emission spectrum in the magnetic field that takes into account the details of the subband structure, the excitonic effects, and the shakeup of the Fermi sea for a localized hole in a valence band. Our goal is to understand the effect of the magnetic field on the FES and how magnetoexcitons associated with higher subbands can lead to strong oscillations in the emission spectrum which are almost periodic in $1/B$.

Let us consider a quantum well in a perpendicular magnetic field B in a symmetric gauge. The magnetic field provides a parabolic confining potential in the plane of the well and all states are localized. The single-particle electron states $|m, n, j\rangle$ in the conduction band are classified by three quantum numbers: the radial quantum number n , the angular momentum number m , and subband quantum number j . The energy spectrum is $E_{n, m, j} = E_j + \hbar\omega_c [n + (m + |m|)/2 + \frac{1}{2}]$, where E_j are subband energies and $\omega_c = eB/Mc$ is the cyclotron frequency, with M being the electron mass. Each subband j forms a separate Landau ladder. The Landau ladders in higher subbands overlap with Landau ladders in lower subbands. This single-particle basis is our final-state basis in the emission process. For interband emission studies the sample must initially contain a hole in the valence

band. We treat the hole as localized at the origin of the plane of the well and at some position z_h in the perpendicular direction. The potential of the positively charged hole is spherically symmetric hence the angular momentum of an electron remains a good quantum number in the presence of the hole. The single-particle states and energies for electrons in the quantum well in the presence of the hole potential are denoted by $|m, \lambda\rangle$ and $E_{m, \lambda}$. This is an initial basis for the calculation of emission. The hole potential introduces a mixing of states with different subband j and radial n quantum numbers. In each angular momentum channel m of the initial basis the energy spectrum is discrete, spaced on the order of cyclotron frequency, and nondegenerate. This is to be contrasted with the situation in the absence of a magnetic field where a continuum of scattering states is associated with each angular momentum channel. Hence the magnetic field effectively reduces the dimensionality of the problem.

Prior to the emission of a photon, the $(N + 1)$ -electron system in the presence of a hole is in the lowest energy state $|f\rangle$. The ground state $|f\rangle$ is a product of the Slater determinant of initial single-particle states $|m, \lambda\rangle$ and a hole state $|h\rangle$. The emission spectrum $E(\omega)$ involves the emission of a photon with frequency ω with simultaneous annihilation of a valence hole and one of the electrons from the conduction band. The annihilation of the hole changes the potential seen by all electrons in the conduction subbands which makes the transition a many-body effect. The emission spectrum $E(\omega)$ is given by a Fourier transform of the real-time current-current correlation function $E(t)$: $E(\omega) = 2 \operatorname{Re} \int_0^\infty dt e^{-i\omega t} E(t)$. The current-current correlation function $E(t)$ is given by^{1, 10–12}

$$E(t) = \sum_{m\lambda, m'\lambda'} M_{m\lambda} \langle f | e^{iHt} a_{m\lambda}^\dagger c^\dagger e^{-iHt} a_{m'\lambda'} c | f \rangle M_{m'\lambda'} . \quad (1)$$

Here $a_{m, \lambda}^\dagger$ creates a conduction-band electron in a state $|m, \lambda\rangle$ with energy $E_{m, \lambda}$ and c^\dagger creates a hole in a state $|h\rangle$ with energy ω_h . The $M_{m\lambda} = P_{vc} \langle m, \lambda | h \rangle$ is the interband transition-matrix element, P_{vc} is an interband momentum matrix element, and $\langle m\lambda | h \rangle$ is the overlap between the electron and hole states. Only zero angular momentum states contribute to emission: $M_{m\lambda} = M_\lambda \delta_{m, 0}$.

We shall omit the angular momentum index m whenever only zero angular momentum states are involved.

The dynamics of the switching off of the hole potential during the emission process is incorporated in the Mahan–Nozières–De Dominicis (MND) Hamiltonian:¹

$$H = \sum_{\lambda, m} E_{m\lambda} a_{m\lambda}^\dagger a_{m\lambda} + (c^\dagger c - 1) \sum_{m\lambda, \lambda'} V_{\lambda, \lambda'}^m a_{m\lambda}^\dagger a_{m\lambda'} + \omega_h c^\dagger c. \quad (2)$$

The potential $V_{\lambda, \lambda'}^m$, to be specified later, scatters electrons between different electron states after the hole has vanished. Integrating out the hole degree of freedom in Eq. (1) gives the current-current correlation function $E(t)$ in terms of matrix elements of the final-state Hamiltonian H_f and N electron states $|\Psi_\lambda\rangle$:

$$E(t) = e^{i\omega_h t} e^{iE_f t} \sum_{\lambda, \lambda' < \mu} M_\lambda \langle \Psi_\lambda | e^{-H_f t} | \Psi_{\lambda'} \rangle M_{\lambda'}. \quad (3)$$

H_f is the final-state Hamiltonian with a repulsive ($-V$) hole potential: $H_f = \sum_{m\lambda, \lambda'} \{E_{m\lambda} \delta_{\lambda, \lambda'} - V_{\lambda, \lambda'}^m\} a_{m\lambda}^\dagger a_{m\lambda'}$, and the electron state $|\Psi_\lambda\rangle$ is a Slater determinant of all occupied states in the Fermi sea except for the zero angular momentum state $|\lambda\rangle$. The missing state was annihilated in the emission process. Hence $|\Psi_\lambda\rangle$ describes a hole in the zero angular momentum state $|\lambda\rangle$ of the Fermi sea. The energy E_f is the ground-state energy of the $(N+1)$ -electron system in the presence of the hole, and μ is the highest occupied level.

The real-time current-current correlation function can be evaluated exactly following the work of Combescot and Nozières.¹¹ The essence is to evaluate the time evolution of the vertex corrections G associated with the hole in the Fermi surface and self-energy C corrections to the “missing” valence-hole potential. This is done in the final basis $|m, n, j\rangle$ for emission, i.e., for Landau states in the absence of the valence hole. The details have been given in Ref. 10 and we only give the final results here:

$$E(t) = e^{iE_f t} e^{i\omega_h t} \sum_{j, n, j', n'} M_{j, n} e^{-iC(t)} e^{+iE_{j, n} t} G_{j, n, j', n'}(t) M_{j', n'}. \quad (4)$$

The matrix elements $M_{j, n}$ are proportional to the overlap of the electron and hole wave functions $M_{j, n} = M_0 \langle 0, n, j | h \rangle$, where M_0 is a constant. The vertex (G) functions satisfy a set of nonlinear differential equations in each individual spin and angular momentum channel m :

$$\begin{aligned} \frac{\partial}{\partial t} G_{j, n}^m(t) = & -iE_{j, n, m} G_{j, n, j', n'}^m(t) \\ & + i \sum_{j'', n''} G_{j, n, j'', n''}^m(t) E_{j'', n''} G_{n'', j'', n', j'}^m(t). \end{aligned} \quad (5)$$

Only the zero angular momentum channel contributes to the emission spectrum. The self-energy corrections $C(t)$ are, on the other hand, determined by vertex corrections in all angular momentum channels as all states are shaken up by the disappearance of the charge of the valence hole:

$$\frac{\partial}{\partial t} C(t) = 2 \sum_{j, n, m} E_{j, n, m} G_{j, n, j, n}^m(t). \quad (6)$$

The factor of 2 comes from the degeneracy of spin as we neglect the Zeeman energy when compared to the cyclotron energy.

An important consequence of working in the final-state basis is that all frequencies $E_{m, n, j}$ of the final basis $|m, n, j\rangle$ contribute to the frequency spectrum of the emission $E(t)$, irrespective of whether they are occupied or empty in the final ground state of the system, i.e., in the absence of the hole. The perturbation of the system created by the hole and the filling of the phase space of initial states in the presence of the hole enters via the initial condition for matrix $G(0)$: $G_{j, n, j', n'}^m(0) = \sum_{\lambda < \mu} \langle m, n, j | m, \lambda \rangle \langle m, \lambda | m, n', j' \rangle$. The summation is over all filled states in the angular channel m in the presence of the hole. The overlap matrix elements $\langle m, n, j | m, \lambda \rangle$ between the initial and final states are solutions of the Wannier equation:

$$\begin{aligned} E_{m, n, j} \langle m, n, j | m, \lambda \rangle + \sum_{j', n'} V_{n, j, n', j'}^m \langle m, n', j' | m, \lambda \rangle \\ = E_{m, \lambda} \langle m, n, j | m, \lambda \rangle. \end{aligned} \quad (7)$$

Here the effective attractive electron-hole interaction matrix elements $V_{n, j, n', j'}^m$ are defined in the final basis.

Let us examine the noninteracting system. For a noninteracting system the initial and final bases sets are the same. The initial condition for the vertex function G is now simply diagonal and given by $G_{j, n, j', n'}^m(0) = \delta_{j, n, j', n'} \Theta(\mu - E_{j, n})$. It is easy to show that the vertex function G does not change in time and the emission spectrum is now given by the contribution from only a few occupied Landau levels in the zero angular momentum channel: $E(t) = e^{i\omega_h t} \sum_{j, n < \mu} M_{j, n}^2 e^{+iE_{j, n} t}$.

The effect of the magnetic field is the quantization of the continuum of states in each angular momentum channel. This introduces a gap in the excitation spectrum and destroys the singularities in the long-time response of the system. This is illustrated by considering the self-energy correction $C(t)$ to second order in the electron-hole interaction using the linked cluster expansion. The relevant part of $C(t)$ which we denote $F(t)$ is written in a standard form as^{1,13}

$$F(t) = -i \int_0^\infty du \frac{R(u)}{u^2} (1 - e^{-iut}). \quad (8)$$

In the single subband case the frequency response function $R(u)$ is given by

$$\begin{aligned} R(u) = \sum_{m, n, n'} |V_{n, n'}^m|^2 f(m, n) [1 - f(m, n')] \\ \times \delta(u - \hbar\omega_c(n' - n)), \end{aligned} \quad (9)$$

where f is the Fermi distribution function and u is the excitation frequency. The frequency response function $R(u)$ is a series of δ functions much like for a valence hole coupled to a boson system.¹ The contribution from the lowest excitation energies is heavily weighted by the u^{-2} term in Eq. (8). In the case of extended states in the

absence of magnetic field the response function $R(u)$ is a linear function of frequency [$R(u)=gu$] and $F(t)$ has a logarithmic singularity for long times: $F(t) \approx -ig \ln(1+i\xi_0 t)$, where g and ξ_0 characterize the excitation spectrum. This form of self-energy leads to a power-law divergence in the valence hole density of states. The application of a magnetic field destroys this behavior and leads to qualitative changes in the hole density of states. It is not possible to extract the information pertaining to the FES from the magnetic-field data.

Before we turn to illustrate in a quantitative way the role of intersubband coupling and magnetic field on the emission spectrum we must specify the form of interactions and matrix elements. Ideally these should be calculated self-consistently including screening as was done for zero magnetic field.¹⁰ The main conclusion from these calculations is that both the optical-matrix elements and electron-hole interaction must be parametrized in a consistent fashion. For a short-range interaction and strongly localized hole we parametrize matrix elements and interaction in terms of electron wave function $\xi_j(z_h)$ evaluated at the position of the hole z_h : $M_{jn} = M_0 h(n) \xi_j(z_h) / l_B$ and $V_{jn, j'n'}^m = -V_0 \delta_{m,0} \xi_j(z_h) \xi_{j'}(z_h)$. The function $h(n)$ determines which Landau levels are optically allowed and l_B is the magnetic length $l_B = \sqrt{\hbar c / eB}$. The electron subband wave functions and energies are calculated for an $\text{In}_x\text{Ga}_{1-x}\text{As}$ quantum well of thickness w sandwiched by thick layers of $\text{Al}_y\text{Ga}_{1-y}\text{As}$ and GaAs. The $\text{Al}_y\text{Ga}_{1-y}\text{As}$ layer is doped with silicon, which donates electrons to the well. The subband wave functions $\xi_j(z)$ and energies E_j are ob-

tained by a variational calculation including confining potentials and Hartree energies. The wave functions for the first two subbands have the form $\xi_1(z) = g_1 z \exp(-b_1 z / 2)$ and $\xi_2(z) = g_2 z (z_0 - z) \exp(-b_2 z / 2)$. The effective potential, the position of energy levels, and wave functions are shown in the inset of Fig. 1. The first subband is filled up to the Fermi energy, which is slightly below the bottom of the second subband. The schematic wave function ξ_h of the hole localized at z_h is also shown. One expects the hole to be localized at the $\text{In}_x\text{Ga}_{1-x}\text{As}/\text{GaAs}$ interface due to the confining potential and interface defects. Another possibility would be the selective doping with acceptors. The optical-matrix elements are proportional to the value of the wave function at the hole position. For holes localized at the GaAs interface matrix elements for transitions to the second subband are negative and much larger than matrix elements for transitions to the first subband. If holes are localized in the node of the second subband wave function, only transitions to the first subband are possible. Hence there is a large tunability in optical properties of these quantum wells.

We show the energy spectrum in the initial (with hole) and final (no hole) basis as a function of the magnetic field in Fig. 1. The energies are all measured in bulk Rydbergs and distance in bulk effective Bohr radii. The width of the well is $w=2$, the Fermi energy is $E_F=7.0$, the subband separation $\Delta=7.1$, and the hole is localized at the InAs/GaAs interface ($z_h=2$). In this configuration the coupling of the hole with the second subband is much larger than the coupling with the first subband ($M_{2,n}/M_{1,n}=-8.0$). The solid line shows the energy spectrum in the final state. The dashed line shows the energy spectrum perturbed by the hole potential. The effect of the attractive electron-hole interaction is the lowering

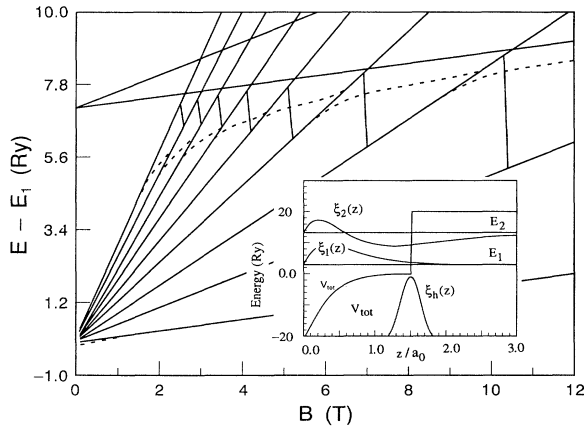


FIG. 1. The energy spectrum $E_{0,n,j}$ of two subbands as a function of the magnetic field B in the absence of the hole potential (solid lines). The thick line shows the position of the Fermi level μ . The dashed line shows the energy levels $E_{0,\lambda}$ deformed by the hole potential. Note the mixing of the $E_{0,0,2}$ level with Landau levels from the first subband. The relevant parameters are well width $w=2$, hole position $z_h=2.0$, strength of electron-hole potential $V_0=1.0$, Fermi energy $E_F=7.0$, intersubband separation $\Delta=7.1$, and the number of Landau levels used $N=11$. Energy is in bulk Rydbergs (1 Ry=5.3 meV). The inset shows a typical potential profile and wave functions for the asymmetric quantum well from Ref. 9.

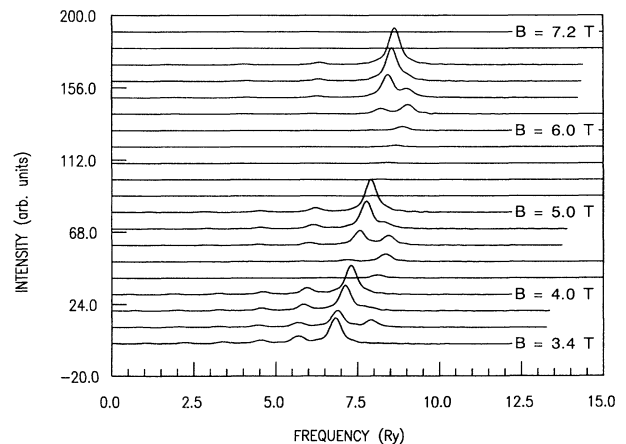


FIG. 2. The emission spectrum $E(\omega)$ for parameters corresponding to Fig. 1 for magnetic field changing from $B=3.4$ to 7.2 T in steps of 0.20 T. Note the large changes in the intensity corresponding to crossing of different subband levels and mixing by the hole potential. The ratio of matrix elements is $M_{n,2}/M_{n,1}=-8.0$ for all n so the coupling to the second subband is much larger than to the first subband.

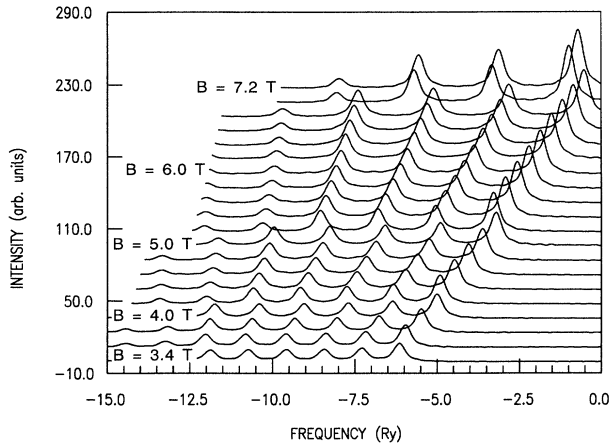


FIG. 3. The emission spectrum $E(\omega)$ for magnetic field changing from $B=3.4$ to 7.2 T in steps of 0.20 T. The ratio of matrix elements is $M_{n,2}/M_{n,1} = -0.24$ for all n so the coupling to the first subband is much larger than to the second subband. There is almost no coupling with intersubband magnetoexcitons. All other parameters as in Fig. 1.

of the energy of the $E_{0,0,2}$ level and its hybridization with Landau levels originating from the first subband. The $|0,0,2\rangle$ state corresponds to the electron in the second subband strongly bound by the hole potential and can be called a resonant (with respect to the lower subband) magnetoexciton. As the magnetic field is removed this level evolves into a Fano resonance.¹⁰ The hybridization takes place when the Landau levels of the first subband $E_{0,n,1}$ intersect the lowest Landau level of the second subband $E_{0,0,2}$. This happens for the special values of the magnetic field B_n satisfying a relation $1/B_n = n\hbar e/\Delta Mc$. In the vicinity of these special values the highest filled Landau level μ associated with the first subband has predominantly the character of the $|0,0,2\rangle$ level. Since the second subband states have much larger matrix elements this has a profound effect on the emission spectrum. In Fig. 2 we show the emission spectrum corresponding to the energy diagram of Fig. 1 over the magnetic-field range $B=3.4-7.2$ T. Each Landau level n couples equally with a hole state, i.e., $M_{n,j} = M_j$, i.e., transitions are non- n -conserving. We see that the spectrum is strongly enhanced at high energies and that the enhancement changes by orders of magnitude as the magnetic field is varied. The changes are almost inversely periodic in $1/B$. The spectrum is quite complex and shows two levels transferring oscillator strength as magnetic field is varied.

None of these phenomena take place if either the coupling to the second subband is reduced or if the Fermi level is well below or above the intersubband separation. We illustrate the effect of intersubband coupling on the emission spectrum in Fig. 3. Here we show the emission spectrum for a hole at $z_h=0.75$. Both the Coulomb coupling and matrix elements for transitions to the first subband are now much larger ($M_{2,n}/M_{1,n} = -0.24$). The emission spectrum is now similar to that obtained by

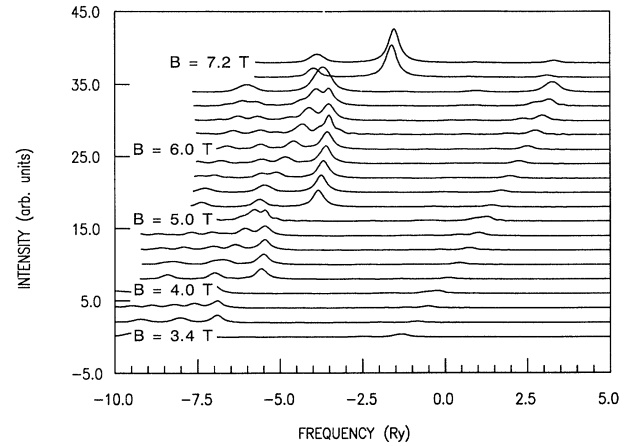


FIG. 4. The emission spectrum $E(\omega)$ for n -conserving optical transitions for magnetic field changing from $B=3.4$ to 7.2 T. The ratio of matrix elements is $M_{0,2}/M_{0,1} = -1.0$ and only $n=0$ transitions are allowed.

Unoyama and Sham.⁸ It shows transitions from occupied Landau levels, enhanced at higher energies, and a shake-up tail at lower energies.

We now consider the situation in which optical transitions conserve also the radial quantum number n . Assuming the hole to be in the lowest energy state with $n=0$ as is expected for a hole with finite mass, only transitions from the $E_{0,0,1}$ electron state are possible. Hence electrons from the vicinity of the Fermi surface cannot contribute to the emission spectrum of the noninteracting system. The emission spectrum representing n -conserving transitions is shown in Fig. 4. We see that the spectrum width no longer reflects the energy width of occupied states. However, due to the mixing of the highest occupied level in the first subband with the $n=0$ empty level in the second subband, there is a spectral feature corresponding to nominally forbidden transitions from the Fermi level.

We should also mention the large (of order of the Fermi energy) relaxation shifts of the emission spectrum in Figs. 2–4 due to the localized hole self-energy. All frequencies are measured from the bare transition frequency ω_h .

In summary, the effect of the magnetic field and resonant magnetoexcitons on the emission spectrum of asymmetric quantum wells is investigated. The main effect of the magnetic field is the quantization of states in each angular momentum channel and the removal of the low-frequency excitation spectrum. The effect of the resonant magnetoexcitons associated with empty subbands is the dramatic increase of electron-photon coupling. These conclusions are drawn from the *exact* solution of a simple multisubband model of noninteracting electrons perturbed by a localized hole. These calculations must be contrasted with the “ladder diagrams” calculations^{6,14} which neglect both dynamical vertex and self-energy corrections. The calculations show that by proper sample engineering large changes in the emission spectrum

are possible. The large enhancement of the emission spectrum is an almost periodic function of the inverse magnetic field. The qualitative conclusions are in agreement with recent experiments by Chen *et al.*⁹ For quantitative agreement with experiment the possibility of the finite hole mass, and the effect of electron-electron and

electron-impurity interactions should be taken into account, especially to understand the correlation of optical and transport data in the quantum Hall regime.

The author would like to acknowledge useful discussions with Arto Nurmikko.

-
- ¹For a review and full references see G. D. Mahan, *Many-Particle Physics* (Plenum, New York, 1981); P. Nozières and C. T. De Dominicis, *Phys. Rev.* **178**, 1097 (1969); J. Gavoret, P. Nozières, B. Roulet, and M. Combescot, *J. Phys. (Paris)* **30**, 987 (1969); S. Doniach and M. Sunjic, *J. Phys. C* **3**, 285 (1970).
- ²C. Delalande, G. Bastard, J. Orgonasi, J. A. Brum, H. W. Liu, and M. Voos, *Phys. Rev. Lett.* **59**, 2690 (1987).
- ³M. S. Skolnick, J. M. Rorison, K. J. Nash, D. J. Mowbray, P. R. Tapster, S. J. Bass, and A. D. Pitt, *Phys. Rev. Lett.* **58**, 2130 (1987).
- ⁴G. Livescu, D. A. B. Miller, D. S. Chemla, M. Ramaswamy, T. Y. Chang, N. Sauer, A. C. Gossard, and J. H. English, *IEEE J. Quantum Electron.* **QE-24**, 1677 (1988).
- ⁵A. E. Ruckenstein, S. Schmitt-Rink, and R. C. Miller, *Phys. Rev. Lett.* **56**, 504 (1986).
- ⁶S. Schmitt-Rink, D. S. Chemla, and D. A. B. Miller, *Adv. Phys.* **38**, 89 (1989); A. E. Ruckenstein and S. Schmitt-Rink, *Phys. Rev. B* **35**, 7551 (1987).
- ⁷J. F. Young, B. M. Wood, G. C. Aers, R. L. S. Devine, H. C. Liu, D. Landheer, M. Buchanan, A. J. SpringThorpe, and P. Mandeville, *Phys. Rev. Lett.* **60**, 2085 (1988).
- ⁸T. Uneyama and L. J. Sham, *Phys. Rev. Lett.* **65**, 1048 (1990).
- ⁹W. Chen, M. Fritze, A. V. Nurmikko, D. Ackley, C. Colvard, and H. Lee, *Phys. Rev. Lett.* **64**, 2434 (1990).
- ¹⁰P. Hawrylak, *Phys. Rev. B* **44**, 6262 (1991); **44**, 3821 (1991).
- ¹¹M. Combescot and P. Nozières, *J. Phys. (Paris)* **32**, 913 (1972).
- ¹²G. D. Mahan, *Phys. Rev. B* **21**, 1421 (1980).
- ¹³P. Hawrylak, *Phys. Rev. B* **42**, 8986 (1990).
- ¹⁴J. F. Mueller, *Phys. Rev. B* **42**, 11 189 (1990); T. Unoyama and L. J. Sham, *ibid.* **39**, 11 044 (1989).